Electrochimica Acta 256 (2017) 211–219

Contents lists available at ScienceDirect

Electrochimica Acta

journal homepage: www.elsevier.com/locate/electacta

Electrodeposition of Cu-Sn alloys from a methanesulfonic acid electrolyte containing benzyl alcohol

L.N. Bengoa[a,b,*], P. Pary[a,b], M.S. Conconi[b,c], W.A. Egli[a]

[a] Centro de Investigación y Desarrollo en Tecnología de Pinturas-CIDEPINT (CICPBA-CONICET), Av. 52 e/121 y 122, B1900AYB La Plata, Argentina
[b] School of Engineering, Universidad Nacional de La Plata, Av.1 y 47, 1900 La Plata, Argentina
[c] Centro de Tecnología de Recursos Minerales y Cerámica-CETMIC (CICPBA-CONICET), Cno. Centenario y 506, B1897ZCA, M.B.Gonnet, Argentina

ARTICLE INFO

Article history:
Received 3 July 2017
Received in revised form 25 August 2017
Accepted 4 October 2017
Available online 5 October 2017

Keywords:
Copper
Tin
Electrodeposition
Methanesulfonic acid
Cyanide-free

ABSTRACT

Deposition of Cu-Sn alloys from a methanesulfonic acid electrolyte containing small amounts of benzyl alcohol was investigated. Polarisation experiments (cylic and linear sweep voltammetry) were carried out using a rotating disc electrode to identify the reduction and dissolution processes that take place in the system and to determine the effect of the solution constituents on them. Potentiostatic deposition was performed onto a rotating cylinder electrode and the resulting deposits were charactised using SEM and XRD. The results showed that co-deposition of copper and tin is possible even at potentials less cathodic than tin discharge potential. The latter was attributed to the underpotential deposition of Sn^{2+} on a copper substrate. Smooth and compact deposits were obtained at various deposition potentials and Cu^{2+} concentrations, with Sn contents between 1.6 - 62.4 wt.%. Several stable phases, such as pure copper, α-CuSn, ε-Cu_3Sn and η'-Cu_6Sn_5 phase, were detected at different operating conditions. Finally, it was found that BA increases the amount of tin in the deposit when Cu^{2+} concentrations in the solution is kept low, especially at high overpotentials. This additive also inhibits the formation of dendrites and reduces surface roughness.

1. Introduction

Cu-Sn alloys have been electrodeposited for over 170 years [1] as protective coatings, mainly due to their wear and corrosion resistance [2–4]. In the last decades, these alloys have found various new applications, such as shape memory materials [5] or lithium-ion battery anodes [6–8], thanks to improvement in deposit morphology, composition and structure [9]. Furthermore, semi-conducting Cu-Sn-S alloys prepared by sulfurisation of electrodeposited Cu-Sn have been recently proposed as absorbers in solar cells [10]. Hence, deposition of Cu-Sn alloys remains a relevant topic for both the academic and industrial communities.

Despite being a rather antique process, Cu-Sn plating technology is still dealing with a major problem: electrodeposition is mostly performed using alkaline cyanide-based electrolytes [2,3,11,12]. These baths are able to produce good quality deposits at affordable current efficiencies but, due to cyanide toxicity [13], they present environmental drawbacks such as an extensive and costly waste treatment process [9]. Consequently, a lot of efforts have been devoted to achieving cyanide-free formulations with the same benefits of the one currently employed. Among the alternatives that have been hitherto studied, it is possible to find sulphate [14–22], sorbitol [23], pyrophospate [24] and citrate based [10] formulations. More recently, choline chloride based deep eutectic solvents have been used to deposit Cu-Sn alloys with promising results [25]. Nonetheless, these solvents present some disadvantages (i.e. higher costs and viscosity [9] than aqueous electrolytes) which have prevented their use at an industrial scale.

In contrast, methane sulfonic acid (MSA) has been gaining acceptance as a supporting electrolyte for deposition of tin [26–29] and tin-alloys [30–32] owing to its excellent metal salts solubility, high conductivity, ease of treatment, stability, a relatively low toxicity and biodegradability [33,34]. In fact, commercial tin plating has been carried out using this electrolyte since the early 1980's [35] and many proprietary MSA-based baths are already available [36–38]. Generally, this formulations include an antioxidant to prevent SnO_2 sludge formation from Sn^{2+} oxidation [39,21] and a grain refiner to obtain smooth and good quality coatings. The

* Corresponding author.
E-mail address: l.bengoa@cidepint.gov.ar (L.N. Bengoa).

https://doi.org/10.1016/j.electacta.2017.10.027
0013-4686/

latter is necessary since tin reduction kinetics are very facile in MSA, which usually leads to disperse or dendritic deposits even at low current densities [40,28]. The increasing popularity of this sulfonic acid makes it an attractive option for the electrodeposition of Cu-Sn alloys, as stated in a recent review by Walsh et. al [30], who also suggested that future work in this field should be focused on the development of MSA-based formulations [9].

Therefore, considering the advantages and several uses (current and potential) of Cu-Sn alloys and the lack of an environment-friendly bath to produce them, in the present work the codeposition of copper and tin from a MSA-based electrolyte was investigated. A commercial formulation used for tin plating containing polyethylene glycol as brightener and a hydroquinone sulfonate salt as antioxidant, was employed as the starting solution. To this electrolyte, small amounts of benzy alcohol (BA) were added which has proved to be beneficial during the deposition of Cu-Sn alloys from phenol sulfonic [41] and sulphate acids [21]. To identify the potential ranges in which individual metal deposition and codeposition take place, cyclic and linear sweep voltammetry was performed. Potentiostatic deposition experiments were carried out to produce Cu-Sn coatings, which were later characterised using SEM, XRD and EDS.

2. Experimental

A 0.54 mol dm^{-3} anhydrous MSA (Aldrich) electrolyte, containing 12 mL dm^{-3} of a polyethylene glycol-based additive (PEG, MW 8000) as brightener and 20 mL dm^{-3} of an antioxidant (hydroquinone sulfonate salt), was used. $SnSO_4$ (Biopack, 90%) was dissolved in this electrolyte to reach a Sn^{2+} concentration of 0.127 mol dm^{-3}, which was chosen according to typical values found in tin-plating industry [36,42] and was left unchanged throughout this work. In contrast, Cu^{2+} ($CuSO_4$ Cicarelli, 100 %) concentration was varied between 0.063 - 0.189 mol dm^{-3} to evaluate the influence of the Cu^{2+}:Sn^{2+} ratio on the codeposition process. In some experiments, 3 mL dm^{-3} of BA were also added to the electrolyte to study its performance as an additive during the electrodeposition of Cu-Sn alloys. All the solutions were prepared using double distilled water.

Cyclic (CV) and linear sweep voltammetry (LSV) were carried out in a three-electrode cell using a 0.041 cm^2 Pt rotating disc electrode (RDE) and a Pt wire as counter electrode. This tests were performed with a computer-controlled (CorrWare2® software) EG&G Princeton Applied Research Potentiostat/Galvanostat (Mod. 273A), using a saturated Ag|AgCl (0.197 V vs NHE) electrode as reference, to which all potentials reported in this study are referred. The potential range considered for these measurements was limited to -0.75 V to 0.70 V. CV curves were recorded at 500 rpm and a scan rate of 20 mV s^{-1}, changing the vertex potential to correlate the anodic and cathodic processes detected. On the other hand, LSV was carried out at various scan rates (1 - 20 mV s^{-1}) and rotation speeds (100 - 1500 rpm). When appropriate, CV stripping efficiency was calculated as the ratio of the charge integrated under the anodic sweep (Q_{an}) to the charge integrated under the cathodic sweep (Q_{cat}) during one voltammetric cycle, using data fitting tools.

Potentiostatic deposition was performed to assess the capability of the MSA electrolyte to produce good quality Cu-Sn coatings. To that end, a low carbon steel rotating cylinder electrode (RCE) 1.6 cm long and 0.9 cm diameter was employed, onto which a pure Cu foil was mounted to serve as substrate. The latter were attached to the steel RCE using a double-sided tape, which was placed only at the edges of the Cu foil to ensure electrical contact between foil and RCE. Prior deposition, Cu substrates were pickled in 100 g dm^{-3} citric acid solution, ground with 1200 grade silicon paper and rinsed with distilled water. For these experiments, a pure copper plate (0.144 cm^2) was used as counter electrode and a saturated Ag|AgCl as reference. The deposition potential was set between - 0.24 V to - 0.54 V using the PAR instrument, while the current density was registered. Plating was carried out until a charge of - 100 C was reached. Once deposition ended, Cu substrates were dismounted for characterisation of their composition and morphology. The Faradaic efficiency (FE) at different potentials was determined by weight difference of the Cu foil before and after electrodeposition. In all potentiostatic experiments, the rotation speed of the working electrode was fixed at 500 rpm.

Surface morphology of the deposits was examined by Scanning Electron Microscopy (SEM) using a Quanta200 FEI microscope, which was also used to evaluate the coatings composition through Energy Dispersive Spectroscopy (EDS). For phase identification, X-ray Diffraction (XRD) patterns were recorded with a Philips 3020 goniometer and a PW 3710 controller with CuKα radiation (λ = 1.54 Å) and a nickel filter. The detector was swept between 10 and 100° with a 0.04° step and 2 seconds per step.Coating thickness was measured from cross section SEM images using Piximetre image analysis software.

3. Results and Discussion

3.1. Polarisation experiments

Fig. 1 shows the typical CV on a Pt electrode for a MSA electrolyte containing Cu^{2+} in the absence and presence of BA. It can be seen that copper deposition starts at a potential of E_{Cu} = - 0.18 V, after which current density increases rapidly reaching a limiting plateau at $E \approx$ - 0.40 V. During the reverse sweep, crossover of the curve corresponding to 3D nucleation is observed [43,44] and, as the potential becomes more anodic than E_{Cu} = 0.05 V, copper dissolution starts leading to the formation of a single peak (A_{Cu}) at E = 0.42 V. Similar results have been previously reported by Low et al. [32] for a MSA electrolyte containing a perfluorinated surfactant. As regards the effect of BA, the voltammograms in Fig. 1 show that this additive slightly inhibits copper deposition process.

For the Sn^{2+} solution (Fig. 2-a), the reduction process begins at E_{Sn} = - 0.40 V, which is in good agreement with Sn deposition onset potentials found in literature [26,32,31]. Further polarisation of the electrode in the cathodic direction leads to the appearance of two peaks: a narrow well-defined peak (C_{Sn1}) at a potential of -0.43 V and a wide wave-like one located at $E \approx$ - 0.55 V. Fig. 2-b shows that current of the first peak increases as the sweep rate increase from 5 to 20 mV s^{-1}, while it is hardly visible at 1 mV s^{-1}. In contrast, the second peak (C_{Sn2}) becomes smaller as sweep rate is increased. A

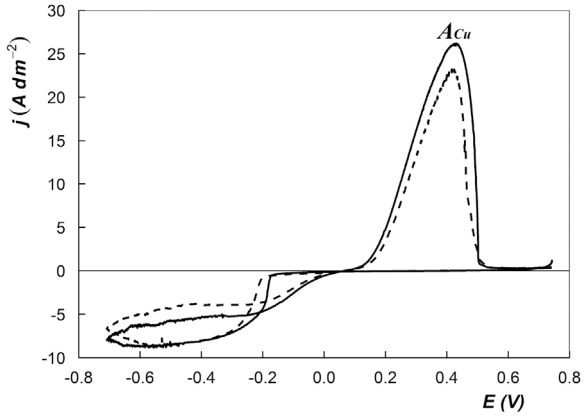

Fig. 1. CV for 0.127 mol dm^{-3} $CuSO_4$ in 0.54 mol dm^{-3} MSA electrolyte (—) without and (- -) with BA. Voltammograms were recorded at 500 rpm and 20 mV s^{-1}.

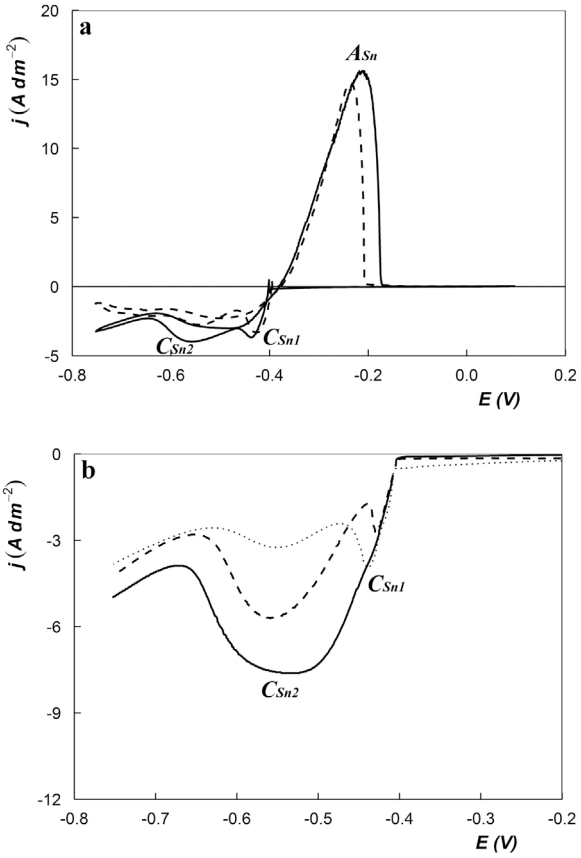

Fig. 2. (a) CV for 0.127 mol dm^{-3} $SnSO_4$ in 0.54 mol dm^{-3} MSA electrolyte (—) without and (- - -) with BA. A scan rate of 20 mV s^{-1} was used and the rotation speed was set at 500 rpm. (b) LSV at 500 rpm for 0.127 mol dm^{-3} $SnSO_4$ electrolyte without BA, recorded at (—) 1 mV s^{-1}, (- - -) 5 mV s^{-1} and (···) 20 mV s^{-1}.

similar behaviour has been previously observed by Low and Walsh [26] in a MSA electrolyte during Sn electrodeposition, and could be attributed to the Sn^{2+} reduction through a two-step mechanism. Considering this, peak C_{Sn1} may be ascribed to the formation of Sn^+ adsorbed species through a slow electrochemical reaction (rate determining step) followed by a faster step ($Sn^+ + e^- \rightarrow Sn$) related to C_{Sn2}. At high sweep rates, only small amounts of Sn^+ precursor are present at the electrode surface and hence development of the second step is limited (decrease in current density of C_{Sn2}). On the contrary, when the potential is swept at low scan rates, a larger amount of Sn^+ species is available at the surface, leading to a depolarisation of the second reaction and a merging of the peaks. After peak C_{Sn2} a decrease in current density is observed likely due to an inhibition effect caused by the presence of an organic additive (PEG 8000) [26]. Finally, at $E <$ - 0.65 V the onset of hydrogen discharge causes a further rise in current density [45]. In the reverse sweep, the CV presents a single stripping peak (A_{Sn}) which corresponds to the two-electron oxidation step of tin. Fig. 2-a also shows that the addition of BA to this electrolyte causes a reduction in the cathodic current density registered for $E <$ - 0.40 V. However, this effect becomes more important at $E <$ - 0.67 V, probably due to the inhibition of the hydrogen evolution reaction on Sn surface [26]. The latter is verified by a slight increase in the stripping efficiency from 0.90 in the absence of BA to 0.93 when this additive is present in the solution. Finally, the decrease in peak A_{Sn} current density provides further evidence of the inhibition effect on Sn^{2+} reduction aforementioned.

LSV of an electrolyte containing both Cu^{2+} and Sn^{2+} is shown in Fig. 3, together with the voltammograms for the individual deposition processes. When both ions are present in the solution,

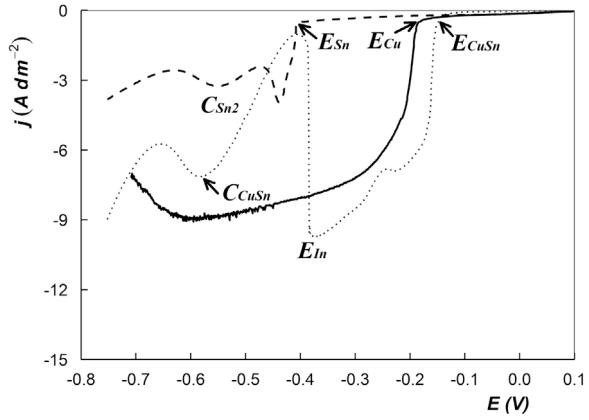

Fig. 3. LSV for (—) 0.127 mol dm^{-3} $CuSO_4$, (- - -) 0.127 mol dm^{-3} $SnSO_4$ and (···) 0.127 mol dm^{-3} $CuSO_4$ + 0.127 mol dm^{-3} $SnSO_4$ in 0.54 mol dm^{-3} MSA, recorded at 500 rpm and 20 mV s^{-1}.

deposition process starts at E_{CuSn} = - 0.15 V, a potential slightly more anodic than that for Cu^{2+} discharge. This depolarisation effect induced by Sn^{2+} has been previously observed in different electrolytes during Cu-Sn electrodeposition [14,46]. As the potential becomes more cathodic, a small shoulder appears at E = - 0.22 V after which current density increases up to a potential of E = - 0.38 V.It is worth noting that the current density for the Cu-Sn system is higher than the sum of the currents for the partial reduction processes in the potential range -0.15 V $< E <$ -0.38 V. However, at E = -0.26 V a change in the voltammogram slope can be appreciated (higher slope). This suggests that underpotential deposition (UPD) of Sn occurs at -0.26 V $< E <$ -0.38 V, a common phenomenon during co-deposition of these two metals from acid electrolytes [41,47,17,15,14]. A sharp drop in current density is registered at E_{In} = - 0.38 V, which has been observed previously by Survila et al. [17,15,48] during co-deposition of Cu and Sn from a sulphate-based electrolyte in the presence of polyethers (like the brightener used in the present work). These authors suggested that the adsorption of surface-active substances onto an unstable free tin phase deposited by an UPD mechanism accounted for this strong inhibition of the reduction process. The latter seems to be a reasonable explanation for this behaviour, especially since E_{In} is equal to the potential at which tin dissolution starts (see Fig. 2-a). Further polarization of the electrode leads to the formation of a peak (C_{CuSn}) at E = - 0.58 V, followed by a second minimum in the voltammogram and a subsequent rise in current density. This behaviour is similar to that observed for Sn electrodeposition (see previous paragraphs) and could be associated with a similar process: simultaneous co-deposition of copper and tin together with hydrogen discharge, followed by a weak adsorption of the brightener (weak inhibition). No significant changes in the electrochemical behaviour were observed after addition of BA to a Cu^{2+}/Sn^{2+} electrolyte. Actually, only a small increase in peak C_{CuSn} current is registered (not shown).

In order to give further insight in the Cu-Sn co-deposition process, CV was performed varying the lower potential limit. The results showed that (Fig. 4) a single stripping peak (A_{CuSn1}), located at $E \approx$ 0.33 V, was observed when the electrode potential is reversed at E = - 0.25 V. Upon shifting the vertex potential to -0.50 V, just a rise in peak A_{CuSn1} current density is registered. However, further polarisation in the cathodic direction (up to E = - 0.75 V) leads to the appearance of a small minimum in cathodic current at E = - 0.32 V, but it does not induce a significant increase in peak A_{CuSn1}. Comparing these results with those for individual Cu deposition (Fig. 1), it may be concluded that the stripping peak A_{CuSn1} corresponds to dissolution of a Cu-rich phase.

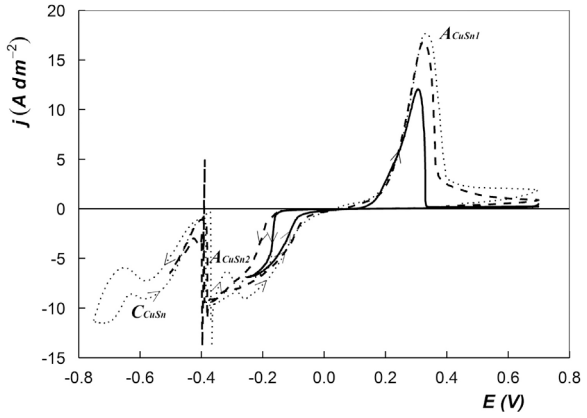

Fig. 4. CV for 0.127 mol dm^{-3} $CuSO_4$ + 0.127 mol dm^{-3} $SnSO_4$ in 0.54 mol dm^{-3} MSA, recorded at 500 rpm and 20 mV s^{-1}. Vertex potential: (—) - 0.25 V, (- - -) - 0.50 V and (···) - 0.75 V.

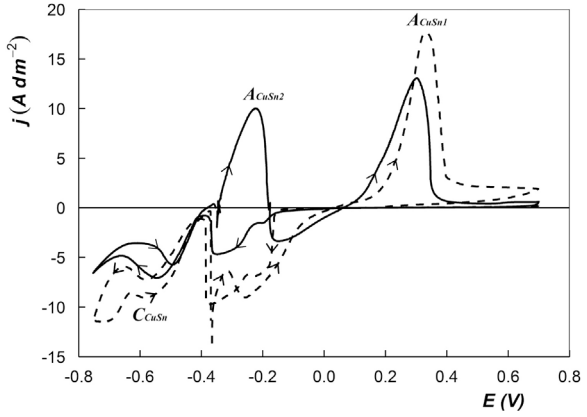

Fig. 5. Effect of Cu^{2+} in the Cu-Sn co-deposition from 0.54 mol dm^{-3} MSA electrolyte: (—) 0.063 mol dm^{-3} $CuSO_4$ and (- - -) 0.127 mol dm^{-3} $CuSO_4$. CV were recorded at 500 rpm and 20 mV s^{-1}. The voltammogram for a Cu^{2+} concentration of 0.189 mol dm^{-3} was not included to improve the visualisation of the features mentioned in the text.

Table 1
Peak and discharge potentials taken from CV and LSV in Figs. 1–5

Electrolyte	Discharge potentials (V)			Cathodic peaks potentials (V)		
	E_{Cu}	E_{Sn}	E_{CuSn}	C_{Sn1}	C_{Sn2}	C_{CuSn}
Cu^{2+}	- 0.18	–	–	–	–	–
Sn^{2+}	–	- 0.40	–	- 0.43	- 0.55	–
Cu^{2+}/Sn^{2+}	–	–	- 0.15	–	–	- 0.58

Electrolyte	Anodic peak potentials (V)			
	A_{Cu}	A_{Sn}	A_{CuSn1}	A_{CuSn2}
Cu^{2+}	0.43	–	–	–
Sn^{2+}	–	-0.22	–	–
Cu^{2+}/Sn^{2+}	–	–	0.33 – 0.50	- 0.32 – - 0.22

CVs recorded at different Cu^{2+} concentrations are presented in Fig. 5. The results indicate that a decrease in copper concentration reduces peak A_{CuSn1} current density, while the minimum observed at E = - 0.32 V develops into a well-defined anodic peak (A_{CuSn2}). Based on its potential, it can be assumed that this second peak is related to the dissolution of Sn-rich phases (see Fig. 2-a). Moreover, at low copper concentrations peak A_{CuSn2} is observed even when potential scan is reversed at E = - 0.50 V. This behaviour confirms

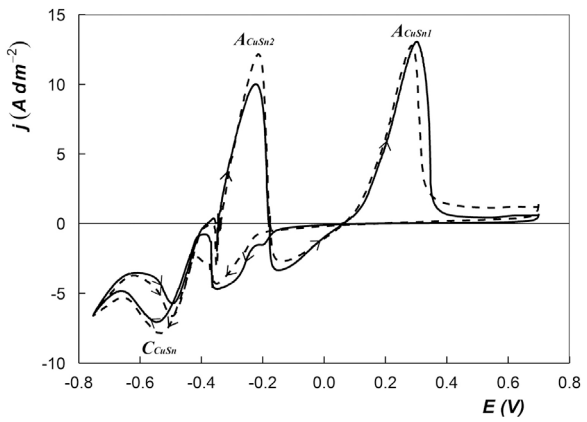

Fig. 6. CV for 0.063 mol dm^{-3} $CuSO_4$ + 0.127 mol dm^{-3} $SnSO_4$ in 0.54 mol dm^{-3} MSA, recorded at 500 rpm and 20 mV s^{-1}, (—) without BA and (- - -) with BA.

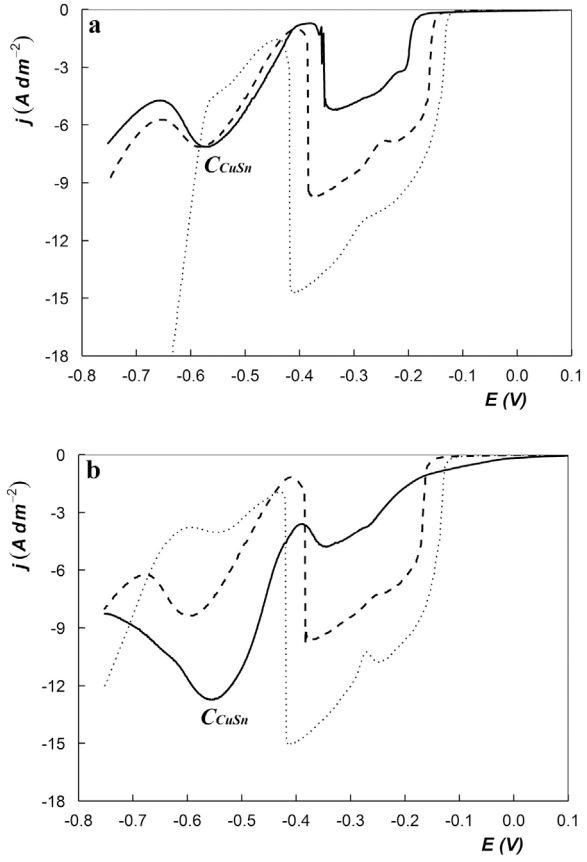

Fig. 7. LSV for a 0.127 mol dm^{-3} $SnSO_4$, 0.54 mol dm^{-3} MSA electrolyte containing (—) 0.063 mol dm^{-3} $CuSO_4$, (- - -) 0.127 mol dm^{-3} $CuSO_4$ and (···) 0.189 mol dm^{-3} $CuSO_4$: (a) without BA and (b) with BA. A scan rate of 20 mV s^{-1} was used and the rotation speed was set at 500 rpm.

the nature of both stripping peaks proposed previously. Another noteworthy feature of these voltammograms is that the position of both peaks depend on the amount of Cu^{2+} in the solution. For peak A_{CuSn1}, its potential changes from 0.30 V to 0.50 V as copper concentration increases from 0.063 to 0.189 mol dm^{-3}, whereas a shift of 100 mV was observed in the case of peak A_{CuSn2}. All peak and discharge potentials mentioned so far are summarised in Table 1. Finally, Fig. 6 shows the effect of BA on the CV for Cu-Sn deposition. It is clearly seen that this additive causes an increase in

peaks C_{CuSn} and A_{CuSn2}, thus promoting deposition of Sn or Sn-rich phases.

The effect of copper concentration on the reduction processes which take place in Cu^{2+}/Sn^{2+} electrolyte was further studied using LSV. Fig. 7 shows that an increase in the amount of Cu^{2+} in the solution shifts E_{CuSn} in the anodic direction, whereas E_{In} becomes more cathodic. Besides, a rise in current density in the potential region between $E_{In} < E <$ - 0.20 V is observed as Cu^{2+} concentration increases. The latter is not surprising since Cu deposition takes place under mixed and mass-transfer control at these potentials (see Fig. 1). It is worth mentioning that this pseudoplateau presents a rather high slope, which can be attributed to the UPD of tin [14,41]. This kind of behaviour was observed both in the presence (Fig. 7-a) and in the absence (Fig. 7-b) of BA. However, at $E < E_{In}$, Cu^{2+} concentration exerts no influence in a solution without BA (Fig. 7), which indicates that this species does not intervene in the reduction process associated with peak C_{CuSn}. In contrast, when the additive is present a decrease in copper concentration leads to a rise in peak's C_{CuSn} current. Comparison of Fig. 7 a and b shows that at low Cu^{2+} concentrations, addition of BA to the solution translates into an increase in the current density for potentials $E < E_{In}$. These results suggest that the effect of BA at high cathodic overpotentials depends on the composition of the film previously deposited. At high Cu^{2+} concentration, a Cu-rich deposit is likely formed in the potential window $E_{In} < E <$ - 0.20 V, with which BA does not interact. Hence, it can be concluded that BA promotes the deposition of Sn or Sn-rich phases but this effect is only relevant at low Cu^{2+}/Sn^{2+} ratios. This fact was considered later to set the composition of the electrolytes for deposition experiments.

Fig. 8 shows LSV recorded at various rotation speeds in the absence of BA. The voltammograms confirm the diffusional nature of the cathodic process in the potential region between $E_{In} < E <$ - 0.20 V, since current density increases with rotation speed in accordance with Levich equation. Furthermore, they indicate that mass transport has an effect on peak C_{CuSn}, which can be related to the diffusional nature of the individual copper reduction process at this potential (see Fig. 2). The same behaviour was observed in the presence of BA (not shown).

3.2. Potentiostatic deposition

Table 2 presents a summary of the deposition conditions together with the composition of the deposits obtained onto copper RCE, determined by EDS. Deposition potentials were chosen

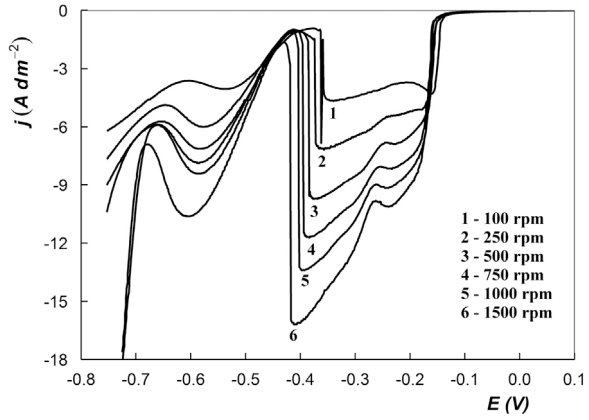

Fig. 8. LSV for 0.127 mol dm^{-3} $CuSO_4$ + 0.127 mol dm^{-3} $SnSO_4$ in 0.54 mol dm^{-3} MSA electrolyte obtained at several rotation speeds between 100 and 1500 rpm. RDE speed is indicated at curve. The scan rate was set at 20 mV s^{-1}.

from LSV experiments in order to obtain Cu-Sn alloy coatings composition and understand better the different features of the voltammograms recorded (see Fig. 3). Considering this, electrodepositon was carried out at a potential close to the onset of Sn UPD (E = - 0.24 V, were a change in the slope of the curve can be seen), at E = - 0.35 V and at a potential close to the sharp drop in current density (E = - 0.40 V). Finally, deposits were obtained at E = - 0.54 V, to identify the electrochemical process taking place at peak C_{CuSn}. Furthermore, Cu^{2+} concentration range used for these experiments was limited to 0.063 - 0.127 mol dm^{-3} based on the results presented in Fig. 7. The data show that Sn content increases as the deposition potential becomes more cathodic and Cu^{2+} concentration in the electrolyte is lowered, as expected based on polarisation experiments carried out in this work and previously reported results [32,31,25,14,49,10,9]. At a copper concentration of 0.063 mol dm^{-3}, addition of BA significantly increases the tin content only at E = - 0.54 V. Otherwise this additive has a limited effect on the deposit composition. In contrast, when Cu^{2+} is raised to 0.127 mol dm^{-3}, deposits obtained in the absence of BA present the same or a slightly higher amount of Sn in their composition. These results are in agreement with voltammetric data. Table 2 also shows that coatings with a Sn content lower than ~ 5 wt.%

Table 2
Experimental conditions and composition for electrodeposits obtained at various potential on a Cu RCE. $SnSO_4$ concentration was kept constant at 0.127 mol dm^{-3} while rotation speed of the electrode was fixed at 500 rpm.

$CuSO_4$ (mol dm^{-3})	E (V)	BA (mL dm^{-3})	Cu content (wt.%)	Sn content (wt.%)	Thickness (μm)	Colour
0.063	- 0.24	–	94.1	4.9	9.2	copper red
		3	94.1	4.9	8.6	copper red
	- 0.35	–	83.8	16.2	8.0	yellow
		3	81.3	18.7	9.7	yellow
	- 0.40	–	77.6	22.4	9.3	yellow
		3	76.3	23.7	9.8	yellow
	- 0.54	–	60.1	39.9	13.8	dark grey
		3	37.6	62.4	14.9	dark grey
0.127	- 0.24	–	97.9	2.1	8.3	copper red
		3	98.5	1.6	7.9	copper red
	- 0.35	–	93.2	6.8	8.5	light red
		3	95.7	4.3	7.9	copper red
	- 0.40	–	91.8	8.2	8.6	light red
		3	94.2	5.9	8.0	light red
	- 0.54	–	78.9	21.1	6.4	yellow
		3	86.6	13.4	9.4	yellow

Fig. 9. Optical images of deposits obtained from a MSA electrolyte containing 0.063 mol dm^{-3} $CuSO_4$ in the presence of BA at various potentials, showing the different colours observed in this study.

present a red colour similar to that of pure copper. As the amount of tin increases, light-red (5 - 9 wt.%) and yellow (13 - 24 wt.%, typical composition of yellow bronze [17,47]) deposits are obtained. Finally, the coatings become dark grey with Sn contents above 40 wt.% (Fig. 9). Current efficiency calculated from gravimetric measurements was found to be higher than 87 % for almost all the deposition conditions considered either in the presence or the absence of BA. For the deposit obtained at E = - 0.54 V in a solution containing 0.127 mol dm^{-3} (without BA), a surprisingly low value of 66 % was estimated probably as a result of H^+ discharge. The latter was not observed when deposition was carried out at the same experimental conditions in the presence of BA, which may inhibit the evolution of H_2. Further studies are needed to completely understand the effect of this additive in the Cu-Sn deposition process.

SEM micrographs of the deposits surface (Fig. 10) show that these are compact and reasonably smooth, with a morphology consisting in small globular protuberances. The only exception is

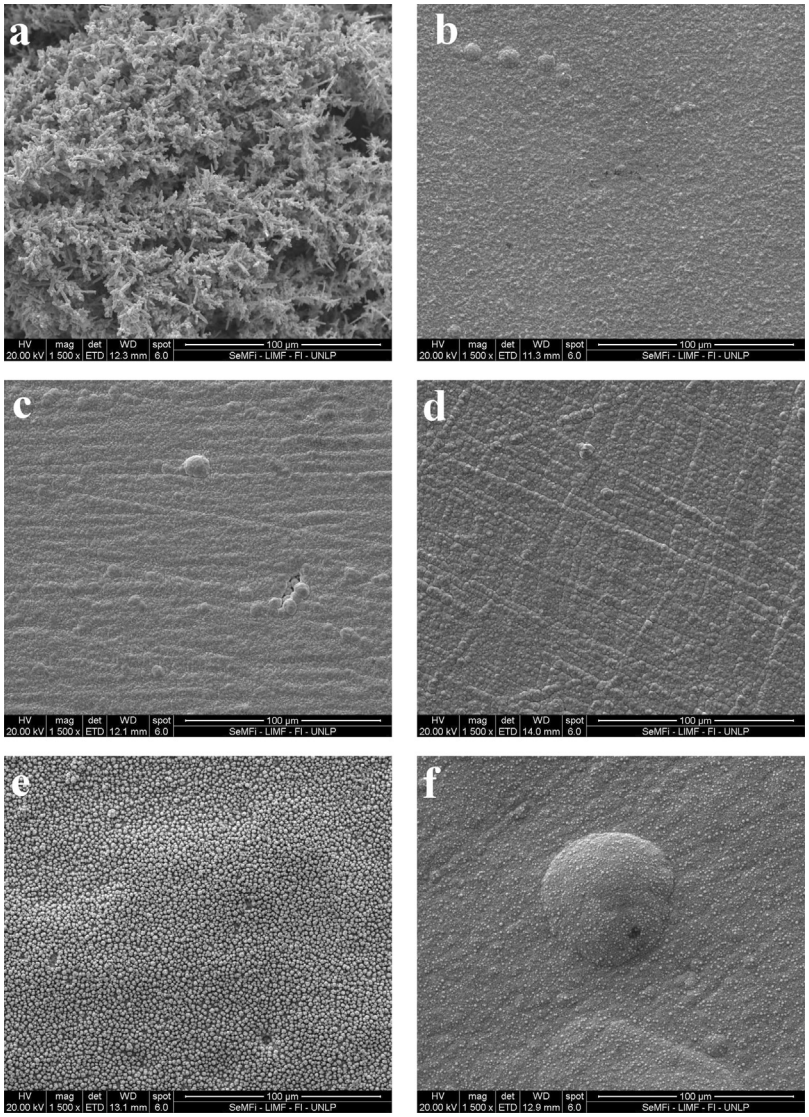

Fig. 10. SEM micrographs (1500 X) of Cu-Sn deposits obtained from a MSA electrolyte containing 0.063 mol dm^{-3} $CuSO_4$ in the absence of BA: (a) - 0.24 V, (c) - 0.35 V and (e) - 0.54 V; with 3 mL L^{-1} of BA: (b) - 0.24 V, (d) - 0.35 V and (f) -0.54 V.

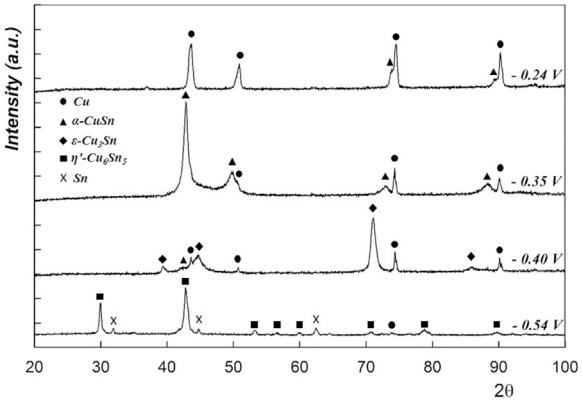

Fig. 11. XRD pattern of Cu-Sn deposits obtained at different potential values from a 0.063 mol dm^{-3} $CuSO_4$ + 0.127 mol dm^{-3} $SnSO_4$ MSA electrolyte, in the absence of BA.

the deposit obtained at E = - 0.24 V and 0.063 mol dm^{-3} $CuSO_4$ in the absence of BA, which is mainly cover with dendrites (Fig. 10-a). At these experimental conditions, the reduction process is likely governed by Cu deposition which is under mass-transfer control (see Fig. 3), which in turn can lead to dendritic growth [50,51]. In the presence of BA, dendrite formation is completely suppressed and a smooth surface morphology develops instead. Furthermore, Fig. 10 also shows that this additive has a brightening/levelling effect which becomes more evident at E = - 0.54 V. Moreover, at this potential deposits obtained in the absence of BA (Fig. 10-e) present some evidence of hydrogen evolution (small pits), which is no longer appreciable when this additive is added to the solution (Fig. 10-f). This indicates that BA suppresses H^+ discharge on a tin-rich surface (see Table 2), in agreement with the results presented for tin deposition (Fig. 2).

XRD diffractograms (Fig. 11) for the samples listed in Table 2 reveal a complex phase composition, which strongly depends on the amount of Sn as expected based on the equilibrium phase diagram (Fig. 12). For tin contents below ~ 13 wt.%, the deposits consist of a mixture of pure copper and fcc α-CuSn (solubility of 15.8 wt.% Sn) in accordance with results reported by other authors [14,47,17]. As the Sn content increases from 13 to 24 wt.%, the ε-Cu_3Sn (orthorombic) becomes the predominant phase whereas the intensities of the peaks corresponding to Cu and the α phase are clearly reduced. Deposits with higher amounts of tin are mainly composed of an hcp-Cu_6Sn_5 (η' phase), together with traces of free-tin and the ε phase. A further increase in Sn content, translates into a rise in the proportion of free-tin in the deposit as well as a decrease in the ε phase amount, which eventually disappears from the XRD patterns. Fig. 11 shows the typical change in phase composition observed in this study when the deposition potential becomes more cathodic, i.e. Sn content increases, in a BA free solution. The same behaviour was observed after addition of BA to the electrolyte (not shown). Finally, it should be mentioned that even though all deposits had a thickness of at least 6.4 μm, the contribution of the substrate to Cu peaks intensity can not be completely disregarded. Hence, only a qualitative analysis of the amount of the different phases present in each sample was performed.

It must be noted that these experiments were carried out potentiostatically, which allows a better control of the stoichiometry of alloys than constant current deposition [9]. However, the latter is the most popular technique in electroplating industry. Hence, to completely assess the capacity of the electrolyte under study to produce good quality Cu-Sn coatings, galvanostatic deposition experiments should be performed. Future investigations will be focused on this issue.

4. Conclusions

The results presented in this work indicate that Cu-Sn alloys coatings can be easily obtained from an industrial MSA-based electrolyte for tin plating after addition of small amounts of $CuSO_4$. Voltammetric data show that co-deposition of copper and tin is even possible at potentials more anodic than E_{Sn}, as a result of the underpotential deposition of Sn. Furthermore, it was observed that formation of free-tin phase might take place at E_{In}, as evidenced by the sharp drop in current density observed at this potential.

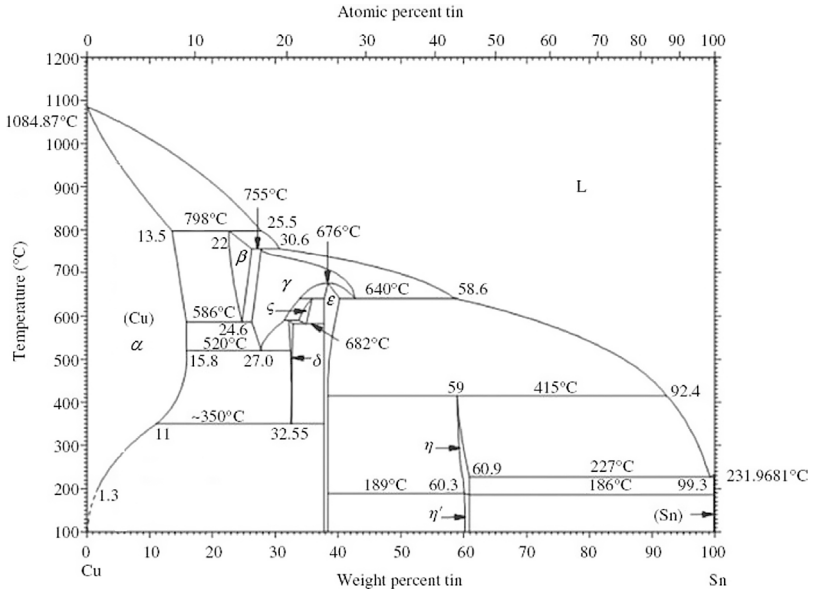

Fig. 12. Cu-Sn equilibrium phase diagram.

BA proved to have a beneficial effect on the electrodeposition of Cu-Sn at low Cu^{2+}/Sn^{2+} ratios. First, even though this additive does not change E_{Cu}, it favours tin deposition making it possible to obtain coatings with a larger amount of this component. It also suppresses hydrogen discharge which increases FE at high cathodic overpotentials. Moreover, BA acts as a brightener/levelling agent avoiding the development of rough or dendritic surface morphologies.

Dense and smooth coatings, containing between 1.6 - 62.4 wt.% of Sn, were deposited at several potentials with acceptable efficiencies (> 87 %). XRD measurements showed that these deposits consist of two or more Cu-Sn phases, and that both the phases and their amount strongly depend on Sn content. Therefore, it can be concluded that the electrolyte considered in this study (MSA electrolyte containing a PEG 8000 as brightener and a hydroquinone sulfonate salt as antioxidant) can be used to electrodeposit Cu-Sn alloys with a wide range of Sn content, which might find applications in different fields.

Acknowledgements

The authors would like to acknowledge the financial support given by Comisión de Investigaciones Científicas de la Provincia de Buenos Aires (CICPBA, Nº 833/14), Consejo Nacional de Investigaciones Científicas y Técnicas (CONICET, PIP Nº 00737) and Universidad Nacional de La Plata (UNLP, Nº 11/I201) for this research. L.N. Bengoa wishes to thank CONICET for a Postdoctoral Fellowship. L.N. Bengoa also appreciates the help rendered by G. Mendivil and N. Alvarez at the laboratory.

References

[1] A. Brenner, Electrodeposition of Copper-Tin Alloys, Academic Press, 1963, pp. 497–543 Ch. 15.
[2] H. Strow, Brass and bronze plating, Met. Finish. 97 (1) (1999) 206–209.
[3] Plating and Electroplating, Vol. 5 of ASM Handbook, ASM International, 1994, 257.
[4] R. Guise, M. Edwards, Tubular member having an anti-galling coating, (2009) .
[5] M. Ceylan, R. Zengin, Shape memory properties and oxidation behaviour of a rapidly liquid quenched Cu-Sn alloy, Journal of Materials Processing Technology 97 (1-3) (2000) 148–152 doi:http://doi.org/10.1016/S0924-0136(99)00381-7..
[6] T. Yamamoto, T. Nohira, R. Hagiwara, A. Fukunaga, S. Sakai, K. Nitta, S. Inazawa, Improved cyclability of Sn-Cu film electrode for sodium secondary battery using inorganic ionic liquid electrolyte, Electrochimica Acta 135 (2014) 60–67 doi:http://doi.org/10.1016/j.electacta.2014.04.159..
[7] A. Kitada, N. Fukuda, T. Ichii, H. Sugimura, K. Murase, Lithiation behavior of single-phase Cu-Sn intermetallics and effects on their negative-electrode properties, Electrochimica Acta 98 (2013) 239–243 doi:http://doi.org/10.1016/j.electacta.2013.03.035..
[8] N. Tamura, R. Ohshita, M. Fujimoto, S. Fujitani, M. Kamino, I. Yonezu, Study on the anode behavior of Sn and Sn-Cu alloy thin-film electrodes, Journal of Power Sources 107 (1) (2002) 48–55 doi:http://doi.org/10.1016/S0378-7753(01)00979-X..
[9] F. Walsh, C. Low, A review of developments in the electrodeposition of tin-copper alloys, Surface and Coatings Technology 304 (2016) 246–262 doi:https://doi.org/10.1016/j.surfcoat.2016.06.065..
[10] G. Heidari, S.M. Mousavi Khoie, M.E. Abrishami, M. Javanbakht, Electrodeposition of Cu-Sn alloys: theoretical and experimental approaches, Journal of Materials Science: Materials in Electronics 26 (3) (2015) 1969–1976 doi:10.1007/s10854-014-2636-1..
[11] A. Afshar, M. Ghorbani, M. Mazaheri, Electrodeposition of graphite-bronze composite coatings and study of electroplating characteristics, Surf. Coat. Technol. 187 (2004) 293–299.
[12] T. Nickchi, M. Ghorbani, Pulsed electrodeposition and characterization of bronze-graphite composite coatings, Surf. Coat. Technol. 203 (2009) 3037–3043.
[13] N. Piccinini, G.N. Ruggiero, G. Baldi, A. Robotto, Risk of hydrocyanic acid release in the electroplating industry, J. Hazard. Mater. 71 (2000) 395–407.
[14] A. Survila, Z. Mockus, S. Kanapeckaite, V. Jasulaitiene, R. Juškenas, Codeposition of copper and tin from acid sulphate solutions containing gluconic acid, J. Electroanal. Chem. 647 (2010) 123–127.
[15] A. Survila, Z. Mockus, S. Kanapeckaite, V. Jasulaitiene, R. Juškenas, Codeposition of copper and tin from acid sulphate solutions containing polyether sintanol ds-10 and benzaldehyde, J. Appl. Electrochem. 39 (2009) 2021–2026.
[16] A. Survila, P.V. Stasiukaitis, Linear potential sweep voltammetry of electroreduction of labile metal complexes-i. background model, Electrochim. Acta 42 (7) (1997) 1113–1119.
[17] A. Survila, Z. Mockus, S. Kanapeckaite, V. Jasulaitiene, R. Juškenas, Codeposition of copper and tin from acid sulphate solutions containing polyether sintanol ds-10 and micromolar amounts of halides, Electrochim. Acta 52 (2007) 3067–3074.
[18] E.P. Barbano, G.M. de Oliveira, M.F. de Carvalho, I.A. Carlos, Copper-tin electrodeposition from an acid solution containing edta added, Surf. Coat. Technol. 240 (2014) 14–22.
[19] Z. Mockus, O. Galdikienė, Cathodic process in copper-tin deposition from sulphate solutions, J. Appl. Electrochem. 24 (1994) 1009–1012.
[20] I. Carlos, C. Souza, E. Pallone, R. Francisco, V. Cardoso, B. Lima-Neto, Effect of tartrate on the morphological characteristics of the copper-tin electrodeposits from a noncyanide acid bath, J. Appl. Electrochem. 30 (2000) 987–994.
[21] G. Medvedev, N. Makrushin, O. Ivanova, Electrodeposition of copper-tin alloy from sulfate electrolyte, Russ. J. Appl. Chem. 77 (7) (2004) 1104–1107.
[22] I. Volov, X. Sun, G. Gadikota, P. Shi, A.C. West, Electrodeposition of copper-tin film alloys for interconnect applications, Electrochimica Acta 89 (2013) 792–797 doi:http://doi.org/10.1016/j.electacta.2012.11.102..
[23] G. Finazzi, E.D. Oliveira, I. Carlos, Development of a sorbitol alkaline Cu-Sn plating bath and chemical, physical and morphological characterization of cu-sn films, Surf. Coat. Technol. 187 (2004) 377–387.
[24] A.N. Correia, M.X. Façanha, P.D. Lima-Neto, Cu-Sn coatings obtained from pyrophosphate-based electrolytes, Surf. Coat. Technol. 201 (2007) 7216–7221.
[25] S. Ghosh, S. Roy, Codeposition of Cu-Sn from ethaline deep eutectic solvent, Electrochimica Acta 183 (2015) 27–36 doi:http://doi.org/10.1016/j.electacta.2015.04.138..
[26] C. Low, F. Walsh, The influence of a perfluorinated cationic surfactant on the electrodeposition of tin from a methanesulfonic acid bath, J. Electroanal. Chem. 615 (2008) 91–102.
[27] C. Low, F. Walsh, The stability of an acidic tin methanesulfonate electrolyte in the presence of a hydroquinone antioxidant, Electrochim. Acta 53 (2008) 5280–5286.
[28] N.M. Martyak, R. Seefeldt, Additive-effects during plating in acid tin methanesulfonate electrolytes, Electrochim. Acta 49 (2004) 4303–4311.
[29] C. Rosenstein, Methane sulfonic acid as an electrolyte for tin, lead and tin-lead plating for electronics, Met. Finish. 88 (1990) 17–21.
[30] F.C. Walsh, C.T.J. Low, Composite multilayer and three-dimensional substrate supported tin-based electrodeposits from methanesulphonic acid, Transactions of the IMF 94 (3) (2016) 152–158 arXiv:https://doi.org/10.1080/00202967.2016.1162399, doi:10.1080/00202967.2016.1162399..
[31] N. Pewnim, S. Roy, Electrodeposition of tin-rich cu-sn alloys from a methanesulfonic acid electrolyte, Electrochim. Acta 90 (2013) 498–506.
[32] C. Low, F. Walsh, Electrodeposition of tin, copper and tin-copper alloys from a methanesulfonic acid electrolyte containing a perfluorinated cationic surfactant, Surf. Coat. Technol. 202 (2008) 1339–1349.
[33] M.D. Gernon, M. Wu, T. Buszta, P. Janney, Environmental benefits of methanesulfonic acid. comparative properties and advantages, Green Chem. 1 (1999) 127–140 doi:10.1039/A900157C..
[34] F.C. Walsh, C.P. de León, Versatile electrochemical coatings and surface layers from aqueous methanesulfonic acid, Surface and Coatings Technology 259 (Part C) (2014) 676–697 doi:https://doi.org/10.1016/j.surfcoat.2014.10.010..
[35] Y. Zhang, Tin and Tin Alloys for Lead-Free Solder, John Wiley & Sons, Inc, USA, 2010, pp. 139–204 Ch. 6..
[36] Y.-H. Yau, The effect of process variables on electrotinning in a methanesulfonic acid bath, J. Electrochem. Soc. 147 (3) (2000) 1071–1076.
[37] W. Zhang, J. Guebey, M. Toben, A novel electrolyte for the high speed electrodeposition of bright pure tin at elevated temperatures, Met. Finish. 109 (1-2) (2011) 13–19.
[38] F. I. Nobel, B. D. Ostrow, D. N. Schram, Tin-lead electroplating solutions US 4,717,460.
[39] D. Thomson, D. A. Luke, C. Mosher, Reducing tin sludge in acid tin plating US 5,378,347.
[40] L.N. Bengoa, W.R. Tuckart, N. Zabala, G. Prieto, W.A. Egli, Tin coatings electrodeposited from sulfonic acid-based electrolytes: Tribological behavior, J. Mater. Eng. Perform. (2015) 1–8.
[41] L.N. Bengoa, W.R. Tuckart, N. Zabala, G. Prieto, W.A. Egli, Bronze electrodeposition from an acidic non-cyanide high efficiency electrolyte: Tribological behavior, Surf. Coat. Technol. 253 (2014) 241–248.
[42] F. I. Nobel, B. D. Ostrow, D. N. Schram, Bath and process for plating tin, lead and tin-lead alloys US 4,565,609.
[43] G. Gunawardena, G. Hills, I. Montenegro, Electrochemical nucleation: Part v. Electrodeposition of cadmium onto vitreous carbon and tin oxide electrodes, J. Electroanal. Chem. 184 (2) (1985) 371–389.
[44] M. Moharana, A. Mallik, Nickel electrocrystallization in different electrolytes: An in-process and post synthesis analysis, Electrochim. Acta 98 (2013) 1–10.
[45] S. Wen, J.A. Szpunar, Nucleation and growth of tin on low carbon steel, Electrochim. Acta 50 (12) (2005) 2393–2399.
[46] L. Skibina, J. Stevanovic, A. Despic, Alsv investigation of the phase composition of electrolytic Cu+Sn alloys, Journal of Electroanalytical Chemistry and Interfacial Electrochemistry 310 (1) (1991) 391–401 doi:https://doi.org/10.1016/0022-0728(91)85274-S..
[47] R. Juškenas, Z. Mockus, S. Kanapeckaite, G. Stalnionis, A. Survila, XRD studies of the phase composition of the electrodeposited copper-rich Cu-Sn alloys, Electrochim. Acta 52 (3) (2006) 928–935.

[48] A. Survila, Z. Mockus, S. Kanapeckaite, D. Braž inskiene, R. Juškenas, Surfactant effects in Cu-Sn alloy deposition, Journal of The Electrochemical Society 159 (5) (2012) D296–D302 arXiv:http://jes.ecsdl.org/content/159/5/D296.full.pdf+html, doi:10.1149/2.084205jes..

[49] A. Survila, Z. Mockus, S. Kanapeckaitė, V. Jasulaitienė, Co-deposition of copper and tin from acidic sulfate solutions containing polyether laprol 2402: The effect of halides, Russian Journal of Electrochemistry 40 (8) (2004) 855–859 doi:10.1023/B:RUEL.0000037952.60589.bd..

[50] K.I. Popov, N.D. Nikolic, General theory of disperse metal electrodeposits formation, Modern Aspects of Electrochemistry, Springer Science+Business Media, New York, 2012, pp. 1–62 Ch. 1..

[51] K.I. Popov, N.V. Krstajic, M.I. Cekerevac, The mechanism of formation of coarse and disperse electrodeposits, Vol. 30, Plenum Press, New York, 1996, pp. 261–312 Ch. 3..